Green approach for an eco-compatible consolidation of the Agrigento biocalcarenites surface

V. Daniele[1], G. Taglieri[1], L. Macera[1], G. Rosatelli[2], J. Otero[3], A.E. Charola[4]

[1] *Department of Industrial and Information Engineering and Economics, University of L'Aquila, 67100 L'Aquila; Tel. 0039 862 434234; Fax 0039 862 434206; *valeria.daniele@univaq.it; giuliana.taglieri@univaq.it; ludovico.macera@graduate.univaq.it*

[2] *Department of Psychological, Humanistic and Territorial Sciences, University of Chieti, Via dei Vestini 31, I-66100 Chieti (CH), Italy; grosatelli@unich.it*

[3] *Materials and Engineering Research Institute, Sheffield Hallam University, Sheffield, S1 1WB, UK; Jorge.Otero@student.shu.ac.uk*

[4] *Museum Conservation Institute, Smithsonian Institution, Washington DC, USA; CharolaA@si.edu*

Abstract. In this paper, we investigate a conservation treatment on different kinds of Agrigento's biocalcarenites, introducing a new non-commercial aqueous nanolime suspension for compatible and eco-friendly extensive applications. This nanolime, here tested for the first time, can be considered a green treatment for both the environment and the health of the conservator. Petrographic, chemico-physical and mechanical investigations of the different biocalcarenites were carried out before and after treatment application. This new nanolime yielded a very promising consolidation effectiveness for all the biocalcarenites, increasing the superficial cohesion and the drilling resistance without significantly altering the stone porosity or the aesthetical features.

Keywords: Agrigento's biocalcarenites; Petrographic characterization; Mineralogical and chemico-physical investigations; Calcium hydroxide nanoparticles; Green and compatible treatments.

1. Introduction

Historical monuments in Mediterranean regions (from Sicily, Italy, to Malta, Cyprus, and Israel) were mainly built from sedimentary soft porous rocks, commonly called calcarenites, which are characterized by a highly porous carbonatic structure. Due to their high porosity, they are vulnerable to progressive deterioration phenomena, which are induced by the combined action of sea spray, sea-waves, and water infiltration. The main consequence of these deterioration processes is the progressive dissolution of the mineral matrix that in the case of calcarenite stone, corresponds to the leaching of calcite. In particular, some publications underline that in the long-term, in continuously water-saturated environments, the calcite of calcarenites is uninterruptedly being dissolved and washed away thus weakening both bonds and grains [1-3], this being the fundamental mechanism affecting the mechanical behaviour of these soft calcareous rocks. This causes an increase in porosity over time, powdering, and a decrease of the mechanical resistance [3-5]. Many studies have focused on finding suitable treatments for the strengthening of weathered calcareous stones. To date, the most common consolidation treatments reported in literature are based on synthetic polymers and other organic materials (i.e. alkoxysilanes, acrylic, epoxy or vinyl resins) which are mainly used as pore fillers [6-8] as well as on inorganic compounds (i.e. lime-based and barium hydroxide-based products and diammonium hydrogen phosphate - DAP) [9, 10]. Although often effective, the organic treatments are characterized by some drawbacks. The main disadvantages are related to health hazards to humans due to VOCs produced by the organic solvents. Additionally, these polymer-based treatments lack physico-chemical compatibility with the original substrate, so that in several cases, can alter, in a drastic way, the colour of the treated stone [9], and their performance decreases significantly over time. In fact, as in the case of TEOS-based (tetraethyl orthosilicate) and silica-precursor consolidant products, they form disordered lattices of tetracoordinated silica, with poor chemical bonding to the calcitic substrates and the tendency to shrink and crack during drying [11]. As concerns inorganic treatments, the traditional lime-based products present a perfect compatibility, but they are generally affected by low penetration depth and slow carbonation, resulting in a limit for

their efficacy as well for a whitening effect on the treated surface [9, 12-13]. Treatments performed with DAP solution, although at now they are promising for the consolidation of carbonatic stones, however they present some drawbacks [10]: 1) metastable calcium phosphate phases more than hydroxyapatite are formed; (2) small unreacted phosphate fractions remain in the stone, requiring additional calcium sources as a second step; (3) non-negligible alterations, mainly in terms of lightness, visible by human eye.

In such context, the application of nanomaterials and nanotechnology can offer the possibility of designing inorganic consolidant products, highly compatible with the original stone substrate. In particular, nanosized $Ca(OH)_2$ dispersions in alcohol or hydro-alcohol mixtures (also called nanolime) are applied as consolidant agents to limestones, lime-mortars, and for calcareous substrates in general [14-17], improving significantly the limitations of the traditional lime treatments [18, 19]. Due to their features, nanolime particles can be considered the best binder to be used in a fully compatible way for the consolidation of all carbonatic substrates, given their total chemical compatibility with the calcitic substrate related to their reaction with atmospheric CO_2 to produce calcium carbonate. Moreover, the higher effectiveness of nanolime treatments, if compared to similar lime-based consolidants, can be ascribed to the small average size of particles that allows a deeper penetration of the nanoparticles into the treated substrates. Furthermore, nanolime dispersions show a high stability thus reducing the formation of undesirable white glazing on the treated surfaces.

As reported in the literature, nanolime treatments are being successfully tested on mural paintings, stuccoes and natural stones, and on all the carbonatic-based substrates where a consolidation treatment is required [16-27]. Nanolime dispersions for conservative treatments, can now be formulated according to several procedures, such as in diols, water-in-oil micro-emulsions, aqueous solutions with or without surfactants, solvothermal reactions or hydro plasma metal reaction [21, 28-31]. Nevertheless, in most of these synthesis processes the final reaction product is rarely pure $Ca(OH)_2$, but it may contains few percentage of contaminants such us residual surfactants, diols or

chlorides. In addition, washing and purification steps are needed to eliminate the by-products and/or organic compounds, leading to low yield of particles and prolonged synthesis times.

In order to overcome the limitations of the current synthesis procedures, we recently patented an original and innovative one-step process that allows to produce pure and crystalline $Ca(OH)_2$ and $Mg(OH)_2$ nanometric particles in few minutes and without intermediate steps, working at room temperature and ambient pressure [17, 32-34]. In particular, the nanolime particles are produced in aqueous dispersions but they can be also dispersed in water/alcohol mixtures, by varying the concentration and solvent to improve the colloidal stability. In addition, the simplicity and the time/energy saving conditions of the method are sufficiently promising to increase the nanolime production from laboratory to an industrial scale, offering the possibility of extensive use of nanolime, such as architectural stone surfaces or historic mortars.

The efficacy of this nanolime for conservation treatments on natural stones has been reported in a previous work, tested preliminary on several irregular specimens of biocalcarenite stones from Agrigento, (Italy) [12]. The obtained results confirmed the high reactivity of the $Ca(OH)_2$ nanoparticles, leading to complete carbonation with the formation of pure calcite in just 30 minutes, working at ambient condition. Although we did not have the possibility to carry out the tests according to standard procedures due to the irregular shape of the samples, results showed that the new calcite formed provided a good superficial consolidation by increasing the superficial cohesion, mechanical resistance and/or of water capillary reduction.

Based on the promising results of these preliminary tests, the aim was to carry out a complete investigation on the effectiveness of our nanolime for conservation treatments on the Agrigento's biocalcarenites, according to standard procedures. The present paper gives a relevant contribution to define and optimize an eco-friendly consolidation treatment that can guarantee compatibility for extensive applications. For the first time, we applied the nanolime particles fully dispersed in water, and this could be considered a direct improvement on the traditional limewater treatments. The

increased regulations on Health and Safety have established that volatile organic compounds emissions (VOCs) produced by alcohol are harmful both to the environment and to human health as well as posing a fire hazard in the early stages [35, 36]. In this context, the use of alcohol based solvents in nanolime can be considered a disadvantage for traditional nanolime treatments when a large scale consolidation treatment is required.

The present paper focuses on the nanolime efficacy in terms of capillary water absorption, increase of the superficial consolidation, and the drilling resistance on different types of Agrigento's biocalcarenites. The study used different application methods and varied dispersion medium (alcohol, water and mixtures of both) for the nanoparticles. For each type of stone, several cubic standard samples were used, and petrographic, mineralogical, chemico-physical and mechanical examinations on treated and untreated specimens of the biocalcarenite stones were also performed. Finally, we studied the nanolime carbonation process of the dispersions to analyse both the kinetics and morphology of the phase transformation of the calcium hydroxide nanoparticles into calcium carbonate.

2. Experimental section

2.1 Formulation of the nanolime dispersions with different solvents

The non-commercial nanolime particles were synthesized in the laboratory, according to our patented procedure, as reported in previous works [32-34, 37]. Three nanolime formulations were prepared, characterized by different solvent mixtures: a) an alcoholic dispersion in pure ethanol (**CH_A** sample); b) a water/ethanol mixture W/A = 50 % (**CH_{50}** sample); c) an aqueous dispersion in pure water, referred to as **CH_W**. The carbonation process of the obtained dispersions was followed by means of X-Ray Diffraction (XRD), taking 0.12 ml of each nanolime sample, depositing on a zero background sample holder (ZBh). The samples were dried in a glass container at a temperature of (20 ± 2) °C and relative humidity of (75 ± 5) %, until complete evaporation of the solvent, that needed about 90, 45

and 15 minutes for **CH_W**, **CH_{50}, CH_A** respectively. Due to the different employed solvent, we observed a higher spread onto the ZBh surface of the alcoholic suspension respect to the aqueous one, determining a less amount of solid exposed to the X-ray beam during the measurement.

In particular, we decided to study the nanolime carbonatation process by setting the RH value at 75% in order to maintain the same conditions used to store the biocalcarenite stones after the treatments. XRD patterns were recorded in the angular range from 10° to 70° 2ϑ, (steps size of 0,026° 2ϑ; time per step 200 sec). Each experimental diffraction pattern was elaborated by the Profile Fit Software, and crystalline phases were attributed by ICSD and ICDD reference databases.

The kinetic stability of the obtained nanolime dispersions was determined by turbidity measurements, analysing their absorbance at λ = 600 nm by using UV/VIS Spectrophotometer (*Lambda 2 Perkin-Elmer*) for 20 minutes. Before the test, the nanolime formulations were put into an ultrasonic bath (*Ultra Sonik 300*) in order to reduce the nanoparticles agglomeration. The KS % is measured in function of time and it is calculated using the following formula:

$$KS\ \% = 1 - [(A_0 - A_t)/A_0] \times 100$$

where A_0 is the starting absorbance and A_t the absorbance at time t [12]. The relative kinetic stability (KS %) decreases as result of the nanoparticle settling; values range from 0 (unstable dispersion) to 100 (not settling of the nanoparticles).

2.2 Chemical and mineralogical characterization of the biocalcarenite stones

Taking into account the visual differences of the available samples in terms of porosity, composition and degree of powdering, five kinds of biocalcarenite samples, named as **A**, **B**, **C**, **D** and **E** respectively, were analysed. These samples were collected from the local quarry of Villaseta (Agrigento, Italy), which present similar characteristics to the ones used for the construction of the Temples [38]. All the samples were appropriately cut to obtain regular cubic specimens (3*3*3 cm^3). A general examination of the structure and texture of the biocalcarenite samples was performed on

148 thin-sections, using polarization-fluorescence microscopy (*PFM, AXIO Scope A1-Zeiss*). Prior to
149 analysis, the samples were dried over-night in an oven at 105 °C to obtain the dry mass, according to
150 the instrumental procedure.
151 The porosity and the pore size distribution of these samples was measured by Mercury Intrusion
152 Porosimetry (MIP) using a *PASCAL 140/240* instrument. A contact angle of 140° was assumed
153 between mercury and the stone. An equilibration time of 30 s was used between each pressure
154 increase step and measurement of the intruded volume. As reported in literature, the MIP is capable
155 of measuring pore diameters ranging from 420 μm to 0.005 μm, (due to the limitations of the
156 operating conditions and the applied method, as well as the simplification of textures and real
157 geometry of pores [39]. In parallel, considering such limitations, two other instruments
158 (*Micromeritics AccuPyc 1330 and GeoPyc 1360*) were also used.
159 The samples were characterized in terms of chemical composition by means of X-Ray Fluorescence
160 spectrometry (XRF, *X Spectro-Xepos III*) and X-Ray Diffraction analysis (XRD, *PANalytical X'Pert*
161 *diffractometer*) using Rietveld refinement. In particular, XRD measurements are carried out on the
162 powder coming from the samples, suitably milled and sieved. XRD patterns were recorded in the
163 angular range from 10° to 70° 2ϑ, (steps size of 0.026° 2ϑ; time per step 400 sec). Each experimental
164 diffraction pattern was elaborated by the Profile Fit Software, and crystalline phases are attributed by
165 ICSD and ICDD reference databases. A quantitative estimation of the phase percent was obtained by
166 means of the Rietveld refinement. X-ray data were fitted using the pseudo-Voigt profile function.
167 Specimen displacement, polynomial coefficients for the background function, lattice parameters,
168 profile parameters, and Gaussian and Lorentzian profile coefficients were refined.

169 *2.3 Eco-compatible treatments with the nanolime formulations*

All biocalcarenite samples were treated by using nanolime dispersions having a $Ca(OH)_2$ concentration of 5 g/l, in order to be able to compare the data to the most commercial nanolime products [18, 20, 23, 40, 41].

The study was started by varying the application procedure, using either spray and brushing, as well as the type of solvent (using **CH_A**, **CH_{50}** and **CH_W** nanolime dispersions), to achieve a treatment that would be effective in terms of consolidation and low-chromatic alteration of the treated surface. For this task, we used the **A** stone because of the higher number of available samples. To define the application procedure which causes the minimum variation in chromatic surface alteration, we selected four cubic specimens (3*3*3 cm^3) of the **A** stone and treated two of them by brush and two by spray. These treatments were performed by using a nanolime dispersed in pure water (**CH_W**) since this would result in a greater surface chromatic alteration due to the higher agglomeration ability of water [41]. The **CH_W** dispersion was applied until stone saturation, by repeating the treatment for about 150 times in the spray application, and for 100 times in the brush one. In both the case, about 100 mg of calcium hydroxide are provided to each stone. During the treatment, the specimens were wiped with a wet cloth to remove the consolidant excess and to reduce surface whitening. Subsequently, the samples were stored for one day at RH = (75 ± 5) % and then they are oven-dried at 60 °C to constant mass. Once established the application procedure, we considered additional cubic specimens (3*3*3 cm^3) of the **A** stone and we treated them by using the three nanolime dispersions, to determine the optimal solvent to be used for the considered stones.

The nanolime treatment on the other types of biocalcarenite stones (**B**, **C**, **D** and **E**, respectively), was undertaken by using the solvent that gave the best treatment effectiveness, i.e., the nanolime particles dispersed in pure water (**CH_W**), as reported below (*Section 3.3*). For this final treatment, we considered three cubic specimens (3*3*3 cm^3) for each stone (**A** to **E**). All samples were treated following the same application procedure as described above.

2.4 Consolidation effectiveness

First, a general examination of the texture and structure variation of the various biocalcarenite stones, before and after the nanolime treatment, was performed by using a stereomicroscope (*SM, Leica Stereozoom S8 APO*). Pores size distribution and open porosity was measured by MIP; the tests were carried out on two samples for each treatment measuring approximately 8x8x8 mm^3, taken from both treated and untreated stones.

Subsequently, the effectiveness of the treatments, in terms of surface consolidation, drilling resistance and reduction of water absorption was evaluated by appropriate tests.

The water absorption by capillarity (WAC), before and after the nanolime treatment, was measured on the cubic samples following the standard procedure [12, 42]. For each sample, we measured the values of the average absorption coefficient at 30 minutes (CA), the amount of absorbed water at the end of the test (Q_f) and the percentage variation of CA and of Q_f before and after treatment (named ΔCA and ΔQ_f, respectively). The drying rate of the biocalcarenite samples, saturated with water, was determined by measuring the weight loss over time, following the standard EN 16322 [43] the absorption and drying tests were performed under controlled laboratory conditions (40% RH, T = 22 °C).

Surface cohesion was estimated by the "Scotch Tape Test" (STT), according to ASTM D3359 [44], and the mean of three tests for each sample was used to evaluate the different treatments. In particular, for each test one strip in the same area was performed referring to literature indications [44, 45].

The consolidation improvement was evaluated using a Drilling Resistance Measurement System (DRMS) from *SINT-Technology* and considering the difference between the resistance of the untreated and treated samples. The DRMS measures the force required to drill a hole at constant rotation (rpm) and lateral feed rate (mm/min). The test was carried out using drill bits of 5 mm diameter, rotation speed of 200 rpm, a rate of penetration of 15 mm/min and penetration depth of 10 mm. The mean value was calculated from 10 measurements. As reported in literature, DRMS is

generally considered the most suitable methodology for quantifying consolidation effectiveness and penetration depth of the consolidant, particularly in soft stones [46].

3. Results and Discussion

3.1 Nanolime dispersions

As previously reported, our patented synthetic process results in pure and crystalline $Ca(OH)_2$ nanoparticles, characterized by a hexagonal lamellar morphology. Each lamella presents a thickness < 10 nm and appears constituted of a self-assembly of primary nanoparticles, crystalline and ≤ 10 nm in size [12, 37].

XRD analyses performed to study the carbonation process, revealed that at RH = (75 ± 5) %, all the nanolime dispersions showed a complete carbonation resulting in pure calcite ($CaCO_3$), regardless of the solvent used and the evaporation rate, denoting a great reactivity of this nanolime particles (Figure 1), as also elsewhere reported [27, 37]. Moreover, the complete conversion of $Ca(OH)_2$ into pure calcite is of fundamental importance also for the durability of the treatment, because it guarantees a perfect compatibility with the substrate from a structural and morphological point of view [37].

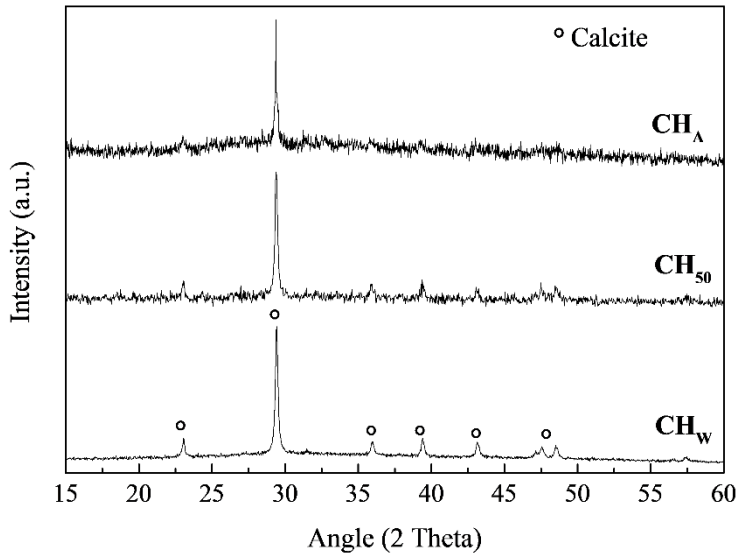

Figure 1. XRD spectra related to the analysis of the carbonation process (RH 75%) of the different nanolime dispersions used for the treatments (Calcite, ICSD #98-015-8258).

From the kinetic stability measurements, we observed that all the dispersions remained stable during the first 5 minutes (Fig. 2). Then, while **CH_A** continued to be stable for the length of the test, both **CH_W** and **CH_{50}** showed a slow settling process, with a KS reduction up to 10% in the first 10 minutes; nonetheless, this gave sufficient time to guarantee an appropriate application of the treatments. As reported in literature, the application of dispersions with lower stability is considered more effective on substrates with very fast moisture transport properties. In fact, the lower stability of the dispersions can limit back-migration of the particles to the drying surface, thus favouring their precipitation in depth and improving the consolidation effect [47].

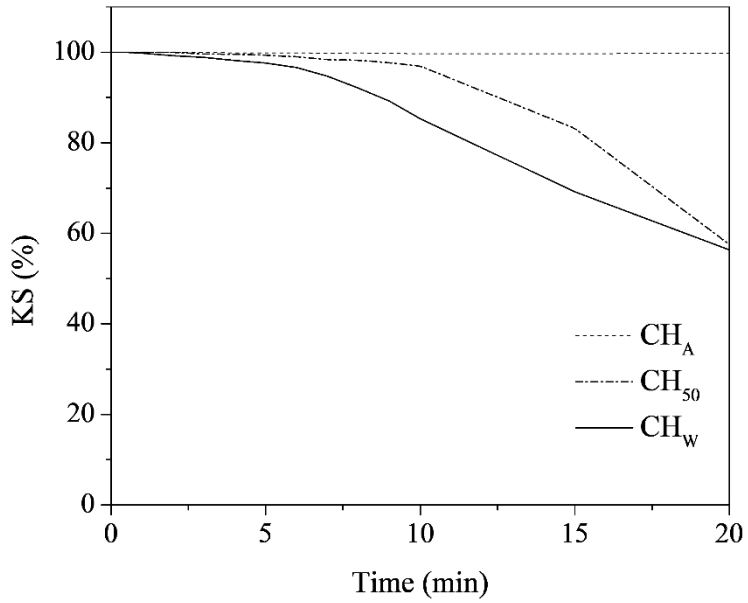

Figure 2. Kinetic stability measurements (KS) versus time, (at λ = 600 nm), for the different nanolime dispersions.

3.2 Biocalcarenite stones

Observation of thin sections, as shown in Figs. 3-5, confirmed that the stone samples belong to the Agrigento Formation of Early Pleistocene age. The formation was composed of medium to coarse-grained bioclastic packstone and grainstone/rudstone, locally lumachella beds, interbedded with a heterogeneous sequence of clay, sandy clays and sands [48]. The calcarenites showed parallel or cross lamination internal structures; they were hybrid, having variable content of terrigenous clasts (1%-50% in volume) mixed with bioclasts. The terrigenous elements were well-rounded quartz and

quartzites of igneous and metamorphic origin. The bioclasts were mainly of pelecypods (Ostrea), bryozoan, red algae (Rhodophyta), fragments of echinoderms, as well as of gastropods. Benthic micro-foraminifera such as Globigerinidae, were also frequent, whereas macro foraminifera, such as nummulites, were rare. Generally, the clasts were cemented by sparry or drusy calcite. In the literature, the presence of *Cyprina islandica* in some coarse calcarenites is reported. However, in the studied samples this bivalve was not observed.

The **A** stone was a grainstone/rudstone composed of ostrea fragments (Fig. 3*a)*) and calcareous red algae as well as Globigerinidae foraminifera. The terrigenous grains represented by rounded quartz crystals were very rare.

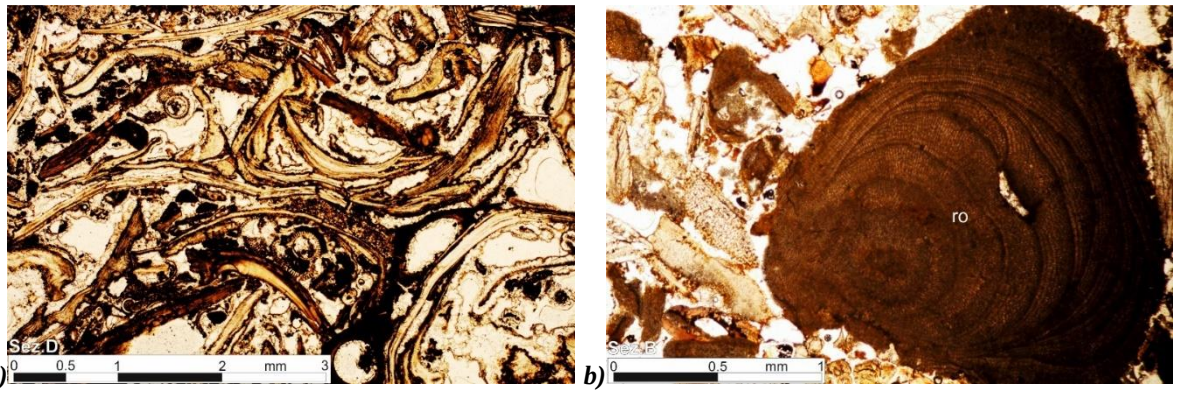

a) ***b)***

Figure 3. ***a)*** Thin section image of **A** stone. Calcite cemented rudstone with dominant bioclasts of ostrea; ***b)*** Thin section image of **B** stone. Red algae rodoficeae (**ro**).

The **B** stone was a packstone containing fragments of Ostrea, bryozoans, red algae and echinoderms (coquina, Fig. 3*b)*). Drusy calcite cements the larger cavities within and between the bioclasts. The matrix does contain little terrigenous fragments, mainly rounded quartz. Few fragments of Globigerinidae micro-foraminifera were observed.

The **C** stone was a hybrid calcarenite with medium to coarse clast size. The terrigenous clasts, mainly quartz of igneous origin, were rounded and their volume does not exceed the 10% (Fig. 4*b)*). The bioclasts were mainly of Ostrea, bryozoans, red algae, echinoderms, macro foraminifera, and only rarely Globigerinidae (Fig. 4*a)*).

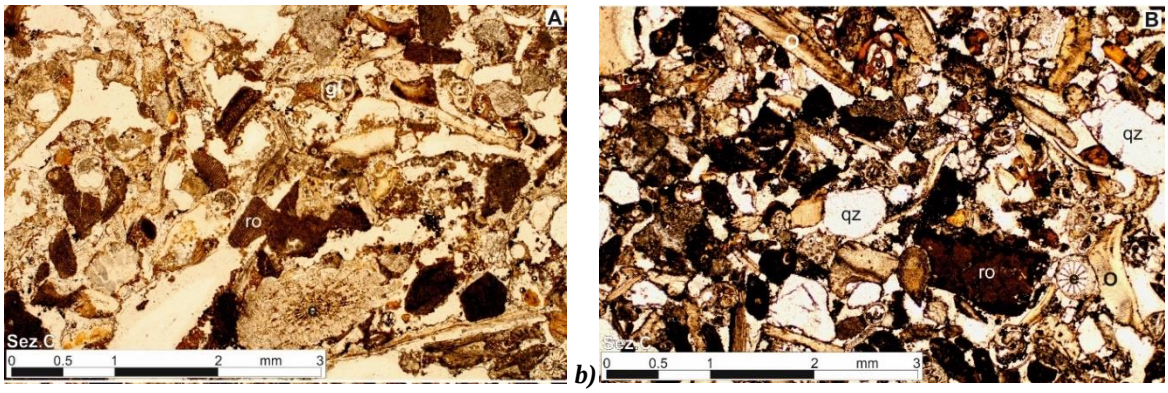

a) ***b)***

Figure 4. Optical microscope images of **C** stone. ***a)*** Calcarenite made of bioclasts: rodoficeae (ro), globigerinidae micro-foraminifers (gl). Fragments of echinoderms (e). ***b)*** hybrid calcarenite with a few rounded quartz clast (qz), bioclasts of *Rhodoficeae* (ro), *Globigerinida*e micro-foraminifers (gl), echinoderms (e) and *Ostrea* (o).

The **D** stone was a hybrid calcarenite with variable content of terrigenous clasts, mainly rounded quartz of igneous, and more rarely, metamorphic origin (Figs. 5*a-b)*). Few fragments of fine-grained polycrystalline quartzite, mixed with bioclastic fragments were observed. The latter were composed of abundant bivalve Ostrea, frequent benthic micro-foraminifera Globigerinidae, rare macro foraminifera *Amphistegina* (Nummulitidae, Fig. 5*c)*), fragments of bryozoans and of echinoderms (Fig. 5*d)*), as well as gastropods (Figs. 5*c-d)*. The larger cavities among the bioclasts were filled with fine-grained quartz sand. The rock forming clasts were cemented by sparry or drusy calcite.

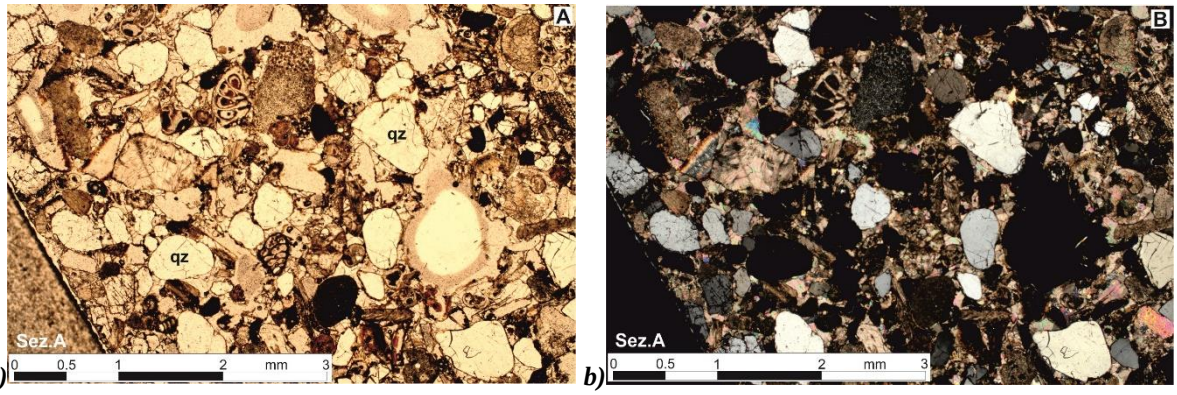

a) ***b)***

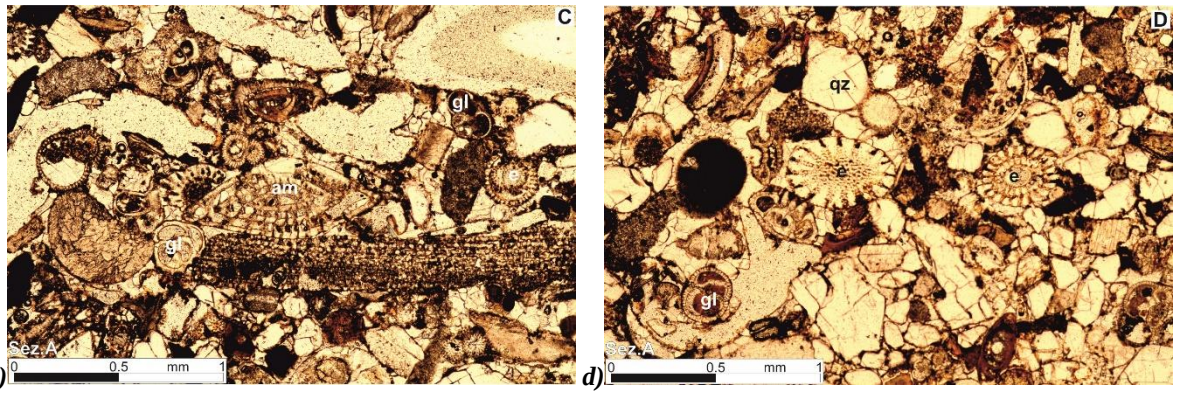

c) *d)*

Figure 5. Optical microscope images of **D** stone: ***a)*** hybrid calcarenite with rounded quartz clasts (**qz**) mixed with bioclasts; ***b)*** cross polarized light view with rounded quartz clast having grey and with I order interference colours. Higher pinkish and yellow interference colours are of the calcite cement; ***c)*** *Globigerinidae* micro-foraminifers (**gl**), macro-foraminifers (*Amphistegina* - **am**), fragments of bryozoa and echinoderms (**e**); ***d)*** rounded quartz crystals (**qz**) fragments of echinoderms (**e**) and *Globigerinidae* micro-foraminifers (**gl**).

From MIP measurements, the stones were characterized by an average porosity, evaluated in the range 0.01-100µm, from 18% to 39%, as reported in Table 1, in agreement with literature results [12, 38]. In particular, as observed from the curves reported in Fig. 6 and specifically from the pore size distribution values (see Table 2), the population of pores were mainly found in the range 10-100 µm.

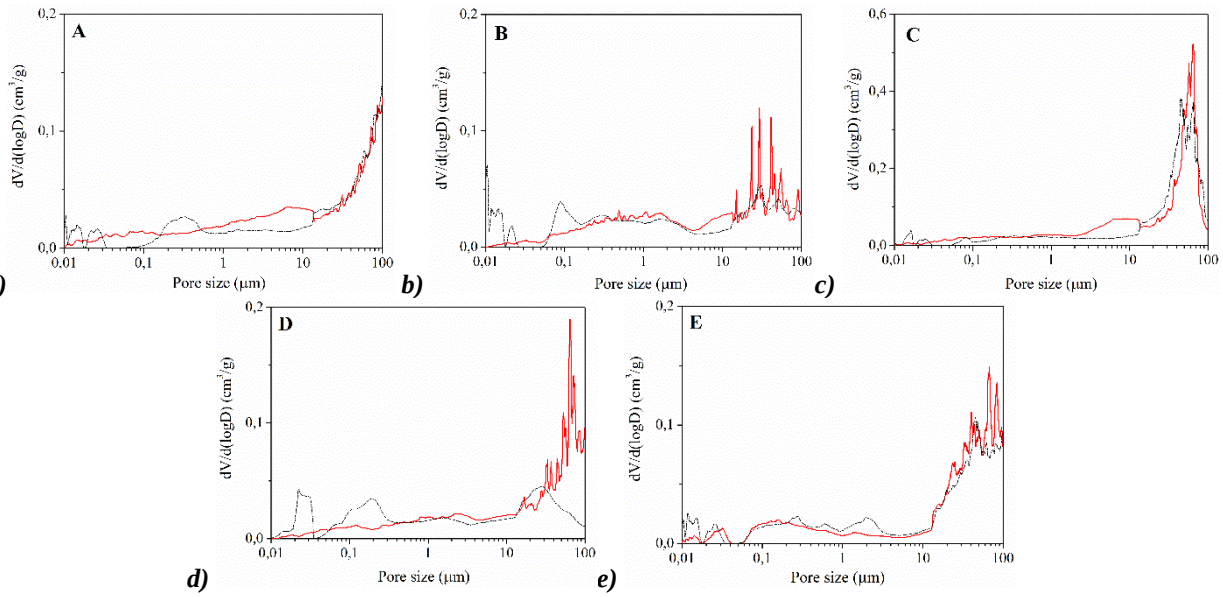

a) ***b)*** ***c)*** ***d)*** ***e)***

Figure 6. Differential volume of intruded mercury versus pore diameter of untreated stones (*continuous lines*). The results referred to the stones, treated by spray with CH_W suspension, were reported by *dot lines*.

From the porosity measurements carried out with AccuPyc/GeoPyc instruments, (see Table 1), we obtained porosity average values from 30% to 41%. These values resulted sometimes higher than MIP results, and this difference could be attributed both to the lowest precision of AccuPyc/GeoPyc instruments respect to MIP and to the presence of closed or larger pores.

The chemical and mineralogical characterization of the different biocalcarenite stones, the XRF and XRD results are reported in Tables 1 and 3, respectively. In particular, the XRD analysis showed that, in all biocalcarenite samples, the main phases were calcium carbonate in form of calcite (from 63 % to 97 %). All biocalcarenite stones presented a low quartz content (from 1.6 % to 8.3 %) apart from **E** stone, which had a 32.7 % of quartz, in agreement with the XRF analysis. In addition, different amounts of aragonite were observed, ranging from 2.1 % for the **A** sample to 31.4 % for the **C** one, but was not detectable in either the **D** or the **E** samples. In the samples D and E the presence of quartz and trace of other mineral such as andradite, gypsum and enstatite (Table 3) is consistent with continental terrigenous detrital input in the depositional basin of the biocalcarenites. The source of these detrital minerals is related to erosion of the inland lithologies composed of limestones, evaporites, silicoclastic deposits and lavas [49].

Table 1. Results of chemical analysis (XRF) and of porosity measurements (from MIP and from AccuPyc/GeoPyc instruments) referred to the different kinds of biocalcarenite samples.

Stone	**XRF**							**MIP**	**Accu/Geo Pyc**
	Ca (%)	Si (%)	Fe (%)	Mg (%)	K (%)	P (%)	S (%)	(%)	(%)
A	38.96	4.76	2.28	0.68	-	0.18	-	26±3	38±2
B	41.97	1.53	2.85	0.90	-	0.14	0.43	18.6±0.4	36.3±0.3
C	39.11	2.30	3.81	1.98	0.18	0.25	0.19	38±1	40±1
D	43.04	2.06	2.45	0.73	-	0.16	-	24±6	34±2
E	35.49	15.5	1.38	0.59	0.27	0.19	-	18±1	30±1

319 **Table 2.** Pore size distribution values of the different kinds of biocalcarenite samples, before and after the nanolime
320 treatment. The results referred to the stones treated by spray ($\mathbf{T_S}$) by using $\mathbf{CH_W}$ suspension.

Stone	Pore diameter ranges (μm)	Porosity (%)	
		UT	T_S
A	100.00 - 39.82	7,19	2,25
	39.82 - 15.85	3,02	2,90
	15.85 - 6.31	1,67	0,65
	6.31 - 2.51	1,49	1,02
	2.51 - 1.00	1,53	1,27
	1.00 - 0.40	1,25	1,07
	0.40 - 0.16	0,81	2,23
	0.16 - 0.06	0,84	1,15
	0.06 - 0.02	0,49	1,80
	0.02 - 0.01	0,12	0,14
B	100.00 - 39.82	3,61	2,366
	39.82 - 15.85	3,413	2,555
	15.85 - 6.31	2,145	0,897
	6.31 - 2.51	1,376	1,238
	2.51 - 1.00	2,313	1,536
	1.00 - 0.40	2,174	1,569
	0.40 - 0.16	1,745	1,723
	0.16 - 0.06	1,046	1,861
	0.06 - 0.02	0,411	0
	0.02 - 0.01	0,173	1,711
C	100.00 - 39.82	17,433	15,965
	39.82 - 15.85	5,204	6,891
	15.85 - 6.31	4,717	1,593
	6.31 - 2.51	2,617	1,146
	2.51 - 1.00	1,779	1,274
	1.00 - 0.40	1,728	1,414
	0.40 - 0.16	1,493	1,301
	0.16 - 0.06	1,406	0,784
	0.06 - 0.02	0,829	0,183
	0.02 - 0.01	0,285	0,741
D	100.00 - 39.82	6,592	6,185
	39.82 - 15.85	2,764	2,777
	15.85 - 6.31	2,864	1,371
	6.31 - 2.51	2,214	1,125
	2.51 - 1.00	1,833	1,164
	1.00 - 0.40	1,362	1,233
	0.40 - 0.16	1,018	1,728
	0.16 - 0.06	1,116	0,049
	0.06 - 0.02	0,813	0,33
	0.02 - 0.01	0,404	0,955
E	100.00 - 39.82	7,803	6,276
	39.82 - 15.85	4,529	3,66
	15.85 - 6.31	0,751	0,723
	6.31 - 2.51	0,459	0,796
	2.51 - 1.00	0,595	1,299
	1.00 - 0.40	0,818	1,056
	0.40 - 0.16	1,266	1,396
	0.16 - 0.06	1,131	0,907
	0.06 - 0.02	0,384	0,29
	0.02 - 0.01	0,26	0,969

321

Table 3. XRD quantitative analyses, by means of Rietveld refinement, carried out on the different kinds of biocalcarenite samples.

Stone	**Calcite** ($CaCO_3$) (*ICSD #98-004-0107*)	**Aragonite** ($CaCO_3$) (*ICSD #98-016-9891*)	**Quartz** (SiO_2) (*ICSD #98-004-2498*)	**Andradite** ($Ca_3Fe_2(SiO_4)_3$) (*ICSD #98-005-2393*)	**Gypsum** $Ca(SO_4)$ $(H_2O)_2$ (*ICSD #98-000-2057*)	**Enstatite** (Mg_2 (Si_2O_6)) (*ICSD #98-008-1130*)
A	89.3%	2.1%	8.3%	0.4%	--	--
B	88.6%	8.7%	1.6%	0.2%	0.8%	--
C	63.0%	31.4%	5.7%	--	--	--
D	97.0%	--	1.9%	1.1%	--	--
E	65.5%	--	32.7%	--	--	1.8%

3.3 Nanolime treatment application on the different biocalcarenites

As previously mentioned we first determined the most suitable application procedure, by applying the **CH_W** dispersion by brush and by spray on selected **A** samples.

As shown in Fig. 7, from a visual inspection, the treatment performed by spray showed no variation in the chromatic surface respect to the untreated material. Conversely, the samples treated by brush, showed a slight whitening effect, which is visible by naked eye, particularly inside the superficial porosity of the sample.

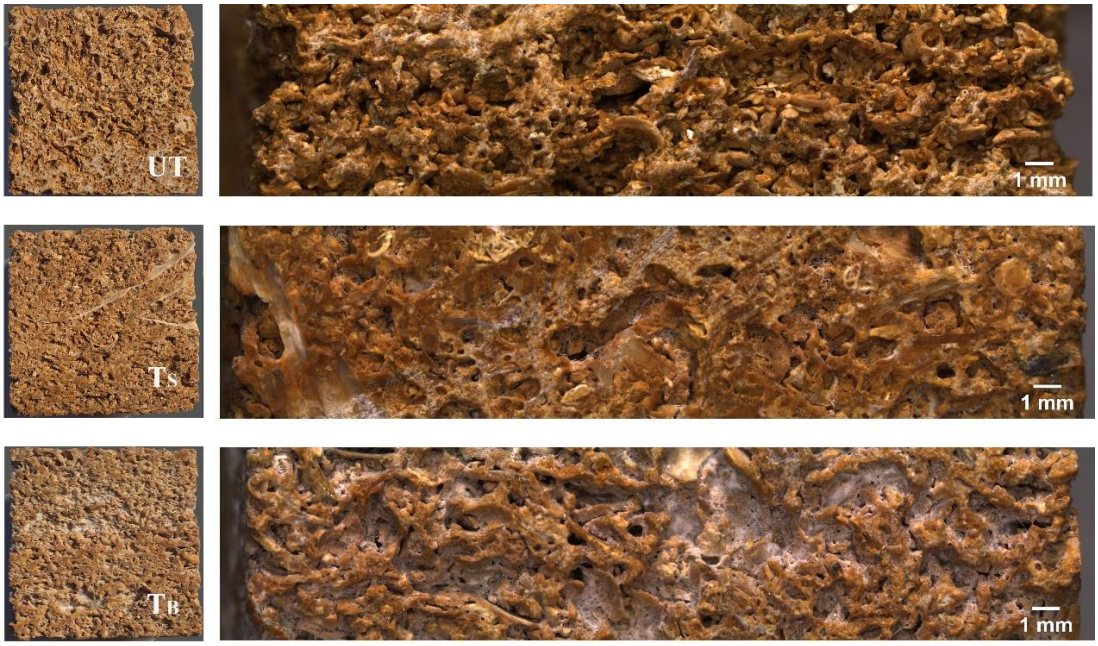

Figure 7. Comparison, in terms of chromatic alteration of the surface, between the untreated sample (UT) and the samples treated by the **CH_W** nanolime applied by spray (T_S) and by brush (T_B). Visual inspections (left images); images from stereomicroscope (right images)

In addition, as reported in Table 4, standard WAC measurements on the **A** samples showed that the nanolime treatments did not particularly affect their behaviour towards water (the ΔQ_f values varied from about 9 to 15 %): however, the absorption kinetics was affected, with a ΔCA variation up to 55 %, between the treated samples (T_B and T_S) and the untreated ones (UT), which suggested the reduction of the pore sizes, as also confirmed by Table 2.

From the STT results, it can be observed that the nanolime treatment carried out by spray yielded the highest increase in surface cohesion, with a reduction of the removed material (ΔM) of 82 %, (Table 4).

Table 4. WAC and STT results performed on **A** cubic samples before and after the nanolime treatment with $\mathbf{CH_W}$ suspension. The treatment was performed by varying the application procedures, by spray (T_S) and by brush (T_B) respectively.

	WAC *			***STT*** *	
	Q_f (mg cm^{-2})	**ΔCA (%)**	**ΔQ_f (%)**	**M (mg cm^{-2})**	**ΔM (%)**
UT	655	53 ± 0.4	9 ± 1	6.83	26 ± 13
T_B	595			5.06	
UT	695	58 ± 4	17 ± 2	19.19	85 ± 9
T_S	575			2.75	

* The results are taken as the average of three measurements for each application procedure

The drilling resistance profiles from DRMS measurements are reported in Fig. 8. The untreated **A** sample presented an average value of resistance of about 7 ± 2 N. After the treatment, carried out by spray, we observed a clear improvement of the resistance with a value of 13 ± 5 N. In contrast, the nanolime treatment applied by brush revealed no significant changes in surface strength compared to the untreated material, as shown in Fig. 8.

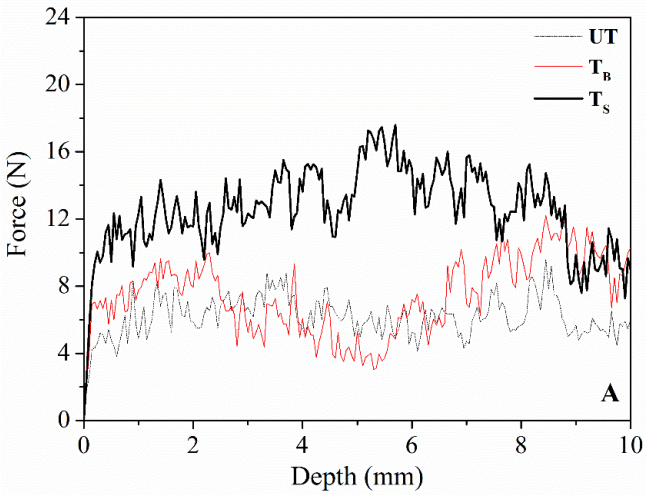

Figure 8. Drilling resistance profiles of biocalcarenite **A** samples: untreated (dot line), treated by brush (continuous lines), treated by spray (marked continuous line).

Considering all the obtained results, it was clear that, applying the nanolime by spray, we obtained a slight higher reduction of water absorbed by capillarity but a significant reduced whitening and higher consolidation efficacy in terms of adhesion and superficial resistance.

Additional cubic samples of the **A** stone were treated by varying the type of solvent in the nanolime dispersions (**CH_W**, **CH_{50}**, **CH_A**). First of all, the microscopic examination of the untreated **A** stone (Fig.9 *a)*) compared to the treated ones, revealed that the nanolime treatments produced no relevant chromatic alterations on the samples surface, independently from the solvent.

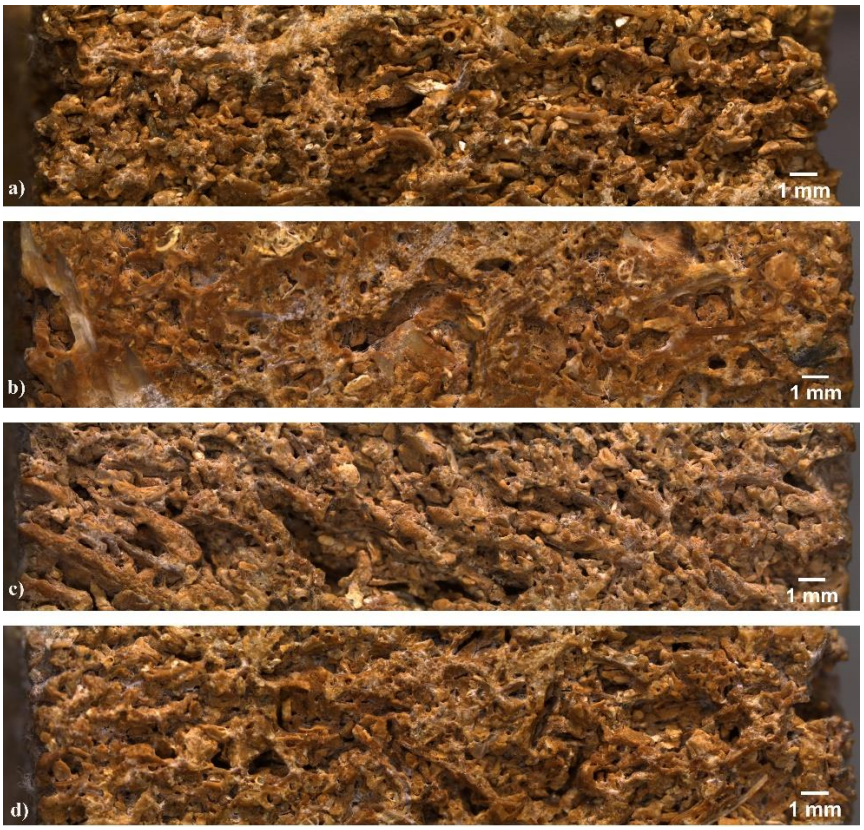

Figure 9. Stereomicroscope image of the **A** stone surface before and after the treatment carried out by spray (5 g/l): *a)* untreated UT; *b)* treated by **CH$_W$** dispersion; *c)* treated by **CH$_{50}$** dispersion; *d)* treated by **CH$_A$** dispersion.

From MIP measurements, carried out after the aqueous nanolime treatment (**CHw**), all the stones showed a general reduction of pores between 1 and 100 µm, together with a tendency to increase a pore population with sizes lower than 0,5 µm (as shown in Fig.6 and in Table 2). A slight reduction of porosity after the treatments was observed for all the stones as well (see Table 6).

These results confirmed that the calcarenite rocks have an important fraction of pores with dimensions >10-100 µm, which were easily accessible to water and so directly involved in the stone durability, as previously reported [50, 51].

WAC and STT tests were performed and the results obtained, taken as the average of three measurements for each nanolime treatment, are summarized in Table 5. We noted that **CH$_W$** and **CH$_A$** showed similar behaviour toward water, except for a slight higher ΔQ_f value for the **CH$_W$** suspension. However, in terms of superficial cohesion only the aqueous dispersion **CH$_w$** revealed a drastic

reduction in the material removed from the surface after the treatment. The ability of the aqueous dispersion to consolidate the surface of the calcarenite stone was confirmed by the DRMS measures too, as shown in Fig. 10. When compared to the alcoholic and to the hydro-alcoholic treatment, the aqueous treatment exhibited a good increase of the superficial resistance up to 10 mm, with a reinforcement particularly marked in the first 2 mm.

This fact can be mainly ascribed to the crucial role of water to promote high efficiency in the carbonation process, [33, 52, 53], so guaranteeing the formation of the new calcite network between the original grains of the stone. In addition, the presence of alcohol can play a detrimental role because of the formation of $CaCO_3$ polymorphs different from calcite, as discussed in several recent literature papers [54, 55].

Table 5. WAC and STT results referred to cubic samples of **A** stone, before (UT) and after the nanolime treatment by spray (T_S). The samples are treated by varying the dispersing medium of the nanolime dispersions.

Nanolime dispersions		***WAC*** *			***STT*** *	
		Q_f (mg cm^{-2})	**ΔCA (%)**	**ΔQ_f (%)**	**M (mg cm^{-2})**	**ΔM (%)**
CH_W	**UT**	695	58 ± 4	17 ± 2	19.19	85 ± 9
	T_S	575			2.75	
CH_{50}	**UT**	725	22 ± 16	6 ± 2	19.19	49 ± 24
	T_S	685			10.18	
CH_A	**UT**	680	60 ± 3	13 ± 2	19.19	37 ± 15
	T_S	590			11.41	

*The results are taken as the average of three measurements for each nanolime treatment

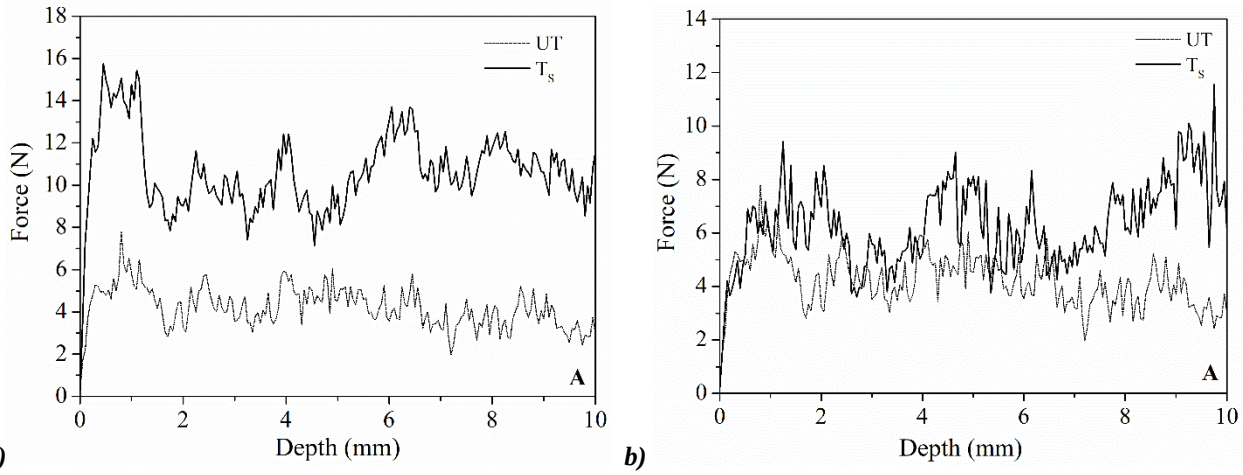

a) ***b)***

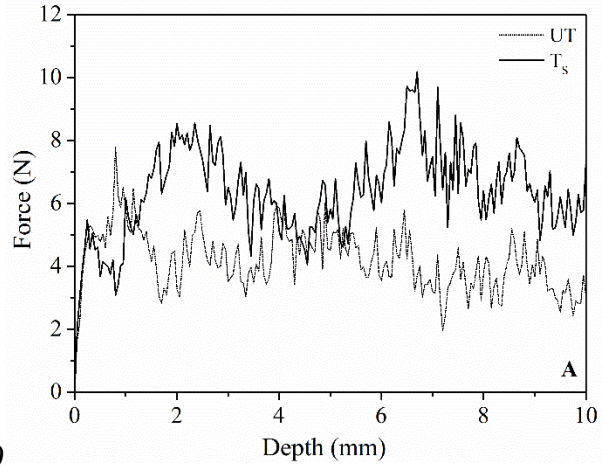

c)

Figure 10. Drilling resistance profiles of untreated (dot line) and treated (continuous lines) **A** stones: ***a)*** treated by **CH_W** suspension; ***b)*** treated by **CH_{50}** suspension; ***c)*** treated by **CH_A** suspension.

Taking into account these results, we treated the other biocalcarenite stones (**B**, **C**, **D** and **E** stones), with the **CH_W** nanolime suspension (applied by spray).

The WAC and STT results, before and after the treatment, are reported in Table 6.

Table 6. MIP, WAC and STT results referred to all the cubic samples of the biocalcarenite stones, before (UT) and after the nanolime treatment by spray (T_S). The samples are treated by using the nanolime suspension in pure water (**CH_W**).

Stone		*MIP*	*WAC* *			*STT* *	
		Porosity (%)	**Q_f (mg cm^{-2})**	**ΔCA (%)**	**ΔQ_f (%)**	**M (mg cm^{-2})**	**ΔM (%)**
A	**UT**	26 ± 3	695	58 ± 4	17 ± 2	19.19	85 ± 9
	T_S	19 ± 1	575			2.75	
B	**UT**	18.6 ± 0.4	286	47 ± 13	13 ± 5	13.87	64 ± 14
	T_S	16 ± 1	247			5.00	
C	**UT**	38 ± 1	881	58 ± 20	15 ± 2	60.94	50 ± 14
	T_S	32 ± 1	743			30.21	
D	**UT**	24 ± 6	418	67 ± 8	12 ± 5	9.27	41 ± 25
	T_S	17 ± 1	367			5.46	
E	**UT**	18 ± 1	405	41 ± 7	17 ± 1	42.75	87 ± 3
	T_S	17 ± 1	335			5.41	

*The results are taken as the average of three measurements for each nanolime treatment

Analysing WAC results, it was confirmed that for all stones, independently of their pore size distribution, the nanolime treatment did not significantly change the amount of water absorbed by capillarity (ΔQ_f average values ranging from 12 to 17 %), but for all the stones it clearly decreased the absorption rate, i.e., the kinetic rise corresponding to ΔCA values. This can be due to the ability

of nanolime to partially fill the pores > 6.31 µm, as observed from the pore size distribution values reported in Table 2. Regarding the STT, for all the stones, the results confirmed the nanolime treatment efficacy in surface consolidation, restoring the cohesion between the superficial grains.

DRMS tests performed on the four types of stones, before treatment, revealed a very different behaviour in terms of mechanical resistance. While **B** and **D** presented an average mechanical resistance from 10 to 20 N in the first 10 mm from the surface (Figs.11 *b), d)*), a scarce resistance characterized **C** and **E** so that most samples broke during the drilling operation itself. In the sporadic cases where the **C** and **E** samples did not break, they presented a very low resistance values (≤ 1 N), (Figs.11 *c), e)*).

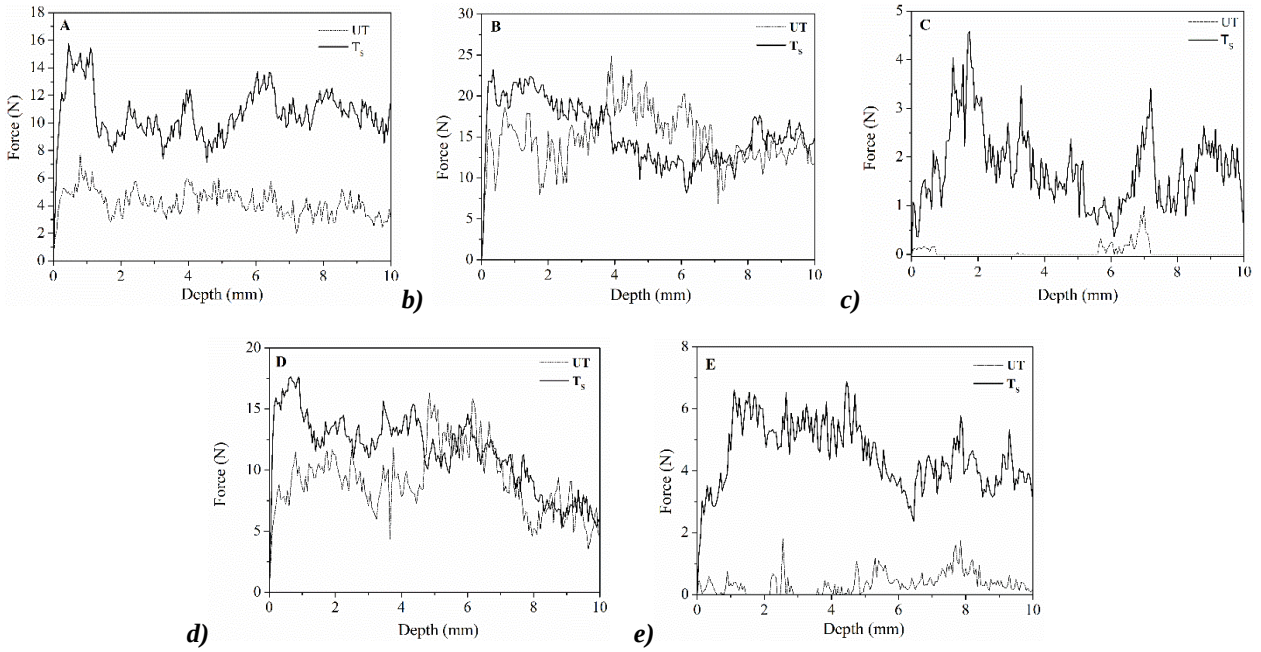

Figure 11. Drilling resistance profiles of untreated (dot line) and treated (continuous lines) biocalcarenite stones

After the nanolime treatments, if **B** and **D** appear only slightly reinforced, **C** and **E** samples did not break during the test reaching average values of resistance from 2 N to 5 N, respectively. The obtained results showed a general increment of resistance in depth, underlining the ability of the nanolime particles, dispersed in pure water, to penetrate up to 1 cm from the surface.

Conclusion

In this study, we present the results of a non-commercial nanolime, produced by an innovative and scalable process, applied as a fully compatible and green consolidation treatment on different types of Agrigento's biocalcarenites. The nanolime treatments' effectiveness was evaluated by means of standard tests, by varying both the application procedures and the dispersing medium, (ethanol, ethanol/water mixture, or pure water), at an established concentration of 5 g/L. First, the highest consolidation effectiveness in terms of lower chromatic changes and higher mechanical properties was achieved using the nanolime suspension applied by spray. Then, we observed that the aqueous nanolime suspension, here employed for the first time, provided a good efficacy with what can be considered "a green treatment". In all the samples, the aqueous nanolime treatment produced only a slight decrease of the water adsorption by capillarity, with a kinetic rise variation up to 67 %, in accordance to the observed reduction of the pores population between 10 and 100 μm. Moreover, the aqueous nanolime treatment increased both the superficial cohesion, with a reduction of material removed from the surface up to 90 %, and the mechanical resistance up to 10 mm from the surface. The possibility of using nanolime dispersions in pure water appears to be very promising in terms of the consolidation effect of a thicker superficial layer, as well as in terms of safety and health issues. The use of water as solvent can overcome some disadvantages such as: a) the problem of the time required for a complete carbonation process, which can require a few hours or less; b) the transformation of $Ca(OH)_2$ nanoparticles into pure calcite (without the formation of other calcium carbonate polymorphs); c) the problem of nanoparticles back migration towards the surface with the solvent (due to the fast evaporation rate of alcohols and to the higher stability of nanolime in alcohol with respect to water); d) the employment of a green product, avoiding the use of organic and volatile compounds, with all the problems connected to the transportation as well as the direct use, especially when the application to very large surfaces are required.

References

449 [1] R.P. Castellanza, R. Nova, Oedometric tests on artificially weathered carbonatic soft rocks,
450 Journal of Geotechnical and Geoenvironmental Engineering 130(7) (2004) 728-739.
451 [2] S. Ghabezloo, A. Pouya, Numerical modelling of the effect of weathering on the progressive
452 failure of underground limestone mines, in: Eurock 2006, Multiphysics Coupling and Long Term
453 Behaviour in Rock Mechanics: Proceedings of the International Symposium of the International
454 Society for Rock Mechanics, Eurock 2006, Liège, Belgium, 9-12 May (2006).
455 [3] M.O. Ciantia et al., Effects of mineral suspension and dissolution on strength and compressibility
456 of soft carbonate rocks, Engineering Geology 184 (2015) 1-18.
457 [4] G.F. Andriani, N. Walsh, Rocky coast geomorphology and erosional processes: a case study along
458 the Murgia coastline South of Bari, Apulia – SE Italy. Geomorphology 87 (2007) 224–238.
459 [5] G.F. Andriani, N. Walsh, The effects of wetting and drying, and marine salt crystallization on
460 calcarenite rocks used as building material in historic monuments. Geochem. Soc. Lond. Spec. Publ.
461 271 (2007) 179–188.
462 [6] P. Tiano et al., Biomediated reinforcement of weathered calcareous stones, Journal of Cultural
463 Heritage 7(1) (2006) 49-55.
464 [7] G.G. Amoroso, V. Fassina, Stone decay and conservation, in: Material Science Monographs 11,
465 Elsevier, Amsterdam (1983).
466 [8] M. Ioele, U. Santamaria, P. Tiano, Comparative study of commercial ethyl silicates and testing in
467 comparison with acrylic microemulsions for the consolidation of matrices carbonates strongly
468 decayed, in: International Congress Silicates in the Conservation (2002) 121-128.
469 [9] M. Matteini et al., Ammonium phosphates as consolidating agents for carbonatic stone materials
470 used in architecture and cultural heritage: preliminary research, International Journal of Architectural
471 Heritage 5 (2011) 717–736.

472 [10] E. Sassoni et al., An innovative phosphate-based consolidant for limestone. Part 1: Effectiveness
473 and compatibility in comparison with ethyl silicate, Construction and Building Materials 102(1)
474 (2016) 918–930.
475 [11] G. Borsoi et al., Evaluation of the effectiveness and compatibility of nanolime consolidants with
476 improved properties, Construction and Building Materials 142 (2017) 385–394.
477 [12] G. Taglieri et al., The biocalcarenite stone of Agrigento (Italy): preliminary investigations of
478 compatible nanolime treatments, Journal of Cultural Heritage, 30 (2018) 92-99.
479 [13] L. Coppola et al., Binders alternative to Portland cement and waste management for sustainable
480 construction–Part 2, Journal of Applied Biomaterials & Functional Materials, (2018), DOI:
481 10.1177/2280800018782852
482 [14] M. Licchelli et al., Nanoparticles for conservation of bio-calcarenite stone, Appl. Phys. A 114
483 (3) (2014) 673-683.
484 [15] D. Chelazzi et al., Hydroxide nanoparticles for cultural heritage: consolidation and protection of
485 wall paintings and carbonate materials, J. Colloid Interface Sci. 392 (2013) 42–49.
486 [16] V. Daniele, G. Taglieri, $Ca(OH)_2$ nanoparticles characterization. Microscopic investigation of
487 their application on natural stones", in: "Materials Characterisation V - Computational Methods and
488 Experiments", A.A. Mammoli, C.A. Brebbia, A. Klemm, Wit press, Southampton, UK (2011) 55-66.
489 [17] G. Taglieri, V. Daniele et al., Eco-compatible protective treatments on an Italian historic mortar
490 (XIV century), Journal of Cultural Heritage 25 (2017) 135-141.
491 [18] D. Costa, J. Delgado Rodrigues, Consolidation of a porous stone with nanolime, in: 12^{th} Int.
492 Congress on Deterioration and Conservation of Stone, New York (USA), 2012.
493 [19] P. Baglioni et al., Commercial $Ca(OH)_2$ nanoparticles for the consolidation of immovable works
494 of art, Appl. Phys. A 114 (2014) 723–732.

[20] A. Zornoza-Indart et al., Consolidation of a Tunisian bioclastic calcarenite: from conventional ethyl silicate products to nanostructured and nanoparticle based consolidants, Construct. Build. Mater. 116 (2016) 188–202.

[21] V. Daniele V. et al., Synthesis of $Ca(OH)_2$ nanoparticles with the addition of TritonX-100. Protective treatments on natural stones: preliminary results, J. Cult.Herit. 13 (2012) 40–46.

[22] V. Daniele, G. Taglieri, Nanolime suspensions applied on natural lithotypes: their influence of concentration and residual water content on carbonatation process and on treatment effectiveness, J. Cult. Herit. 11 (2010) 102–106.

[23] C. Rodriguez-Navarro et al., Alcohol dispersions of calcium hydroxide nanoparticles for stone conservation, Langmuir 29 (2013) 11457–11470.

[24] J. Otero et al., An overview of nanolime as a consolation method for calcareous substrates, Ge-Conservación 1(11) (2017) 71–78.

[25] A. Arizzi et al., Lime mortar consolidation with nanostructured calcium hydroxide dispersions: the efficacy of different consolidating products for heritage conservation, Eur. J. Miner. 27(3) (2013) 311–323.

[26] M. Drdácký et al., A Nano approach to consolidation of degraded historic lime mortars, J. Nano Res. 8 (2009) 13–22.

[27] J. Otero, V. Starinieri, A.E. Charola, Nanolime for the consolidation of lime mortars: A comparison of three available products, Construction and Building Materials 181 (2018) 394-407.

[28] B. Salvadori, L. Dei, Synthesis of $Ca(OH)_2$ Nanoparticles from Diol, Langmuir 17(8) (2001) 2371–2374.

[29] A. Samanta et al., Synthesis of calcium hydroxide in aqueous medium, J. Am.Ceram. Soc. 99 (3) (2016) 787–795.

[30] G. Poggi et al., Calcium hydroxide nanoparticles from solvothermal reaction for the deacidification of degraded waterlogged wood, J. Colloid Interface Sci.473 (2016) 1–8.

520 [31] T. Liu et al., Synthesis and characterization of calcium hydroxide nanoparticles by hydrogen
521 plasma-metal reaction method, Mater. Lett. 64 (2010) 2575–2577.
522 [32] R. Volpe, G. Taglieri, V. Daniele, G. Del Re, A process for the synthesis of $Ca(OH)_2$
523 nanoparticles by means of ionic exchange resin. European patent EP2880101 (2016).
524 [33] G. Taglieri et al., Analysis of the carbonatation process of nanosized $Ca(OH)_2$ particles
525 synthesized by exchange ion process, Proceedings of the Institution of Mechanical Engineers, Part
526 N: Journal of Nanoengineering and Nanosystems, 230(1) (2016) 25-31.
527 [34] G. Taglieri, B. Felice, V. Daniele et al., $Mg(OH)_2$ nanoparticles produced at room temperature
528 by an innovative, facile, and scalable synthesis route, J. Nanopart. Res. 17 (2015) 411-424.
529 [35] M.E. Young, M. Murray, P. Cordiner, Stone consolidants and chemical treatments in Scotland.
530 Edingburgh: Historic Scotland (1999).
531 [36] A. Steinemann, Volatile emissions from common consumer products, Air Qual Atmos Health
532 8(3) (2015) 273-281.
533 [37] G. Taglieri, V. Daniele, L. Macera, C. Mondelli, Nano $Ca(OH)_2$ synthesis using a cost-effective
534 and innovative method: Reactivity study, J.Am.Ceram.Soc. 100 (2017) 5766–5778.
535 [38] C. Bennardo et al., Comparative study of different methods for gap filling appli-cations and use
536 of adhesive on the biocalcarenite surfaces of the “Tempio dellaConcordia” in Agrigento, 9th Intern.
537 Congress on deterioration and conservation of stone, Elsevier, 2000.
538 [39] F.A.L. Dullien, Porous Media – Fluid Transport and Pore Structure, 2nd edn. Academic Press,
539 San Diego, CA. 1992.
540 [40] A. Campbell et al., Calcium hydroxide nanoparticles for limestone conservation: Imbibition and
541 adhesion, Symposium 2011: Canadian Conservation Institute, Ottawa, Canada, 17-21 October
542 (2011).
543 [41] L. Dei, B. Salvadori, Nanotechnology in cultural heritage conservation: nanometric slaked lime
544 saves architectonic and artistic surface from decay, J.Cult. Herit. 7 (2006) 110–115.

545 [42] UNI EN 15801 (2010), Determinazione dell'assorbimento d'acqua per capillarità.
546 [43] EN 16322, European Standard. Conservation of Cultural Heritage - Test Methods -
547 Determination of drying properties. European Committee for Standardization (CEN); October 2013.
548 [44] ASTM D3359-02: "Standard test methods for measuring adhesion by tape test", ASTM
549 International, 10 August, 2002.
550 [45] R. Giorgi et al., A New Method for Consolidating Wall Paintings Based on Dispersion of Lime
551 in Alcohol, Studies in conservations 45 (2000) 154-161.
552 [46] F. Fratini et al., A new portable system for determining the state of conservation of monumental
553 stones, Mater. Struc. 39(286) (2006) 125–132.
554 [47] G. Borsoi et al., Effect of solvent on nanolime transport within limestone: How to improve in-
555 depth deposition. Colloids Surf A 497 (2016) 171–181.
556 [48] V. Cotecchia, G. D'Ecclesiis, M. Polemio, La dinamica dei versanti della Valle dei Templi di
557 Agrigento, Geol. Appl. Idrogeol., XXX(I) (1995) 369-383.
558 [49] P. Di Stefano et al., Note Illustrative della Carta Geologica d'Italia Scala 1:50.000 – Foglio 619
559 S. Margherita in Belice. ISPRA - Regione Sicilia (2013) 192.
560 [50] G.F. Andriani, N. Walsh, Physical properties and textural parameters of calcarenitic rocks:
561 qualitative and quantitative evaluations, Eng. Geol. 67 (2002) 5–15.
562 [51] J.E. Lindqvist, U. Åkesson, K. Malaga, Microstructure and functional properties of rock
563 materials, Mater. Charact. 58 (2007) 1183–1188.
564 [52] F.M.A. Henriques, A.E. Charola, Comparative study of standard test procedures for mortars, In:
565 8th International Congress on Deterioration and Conservation of Stone, Berlin (1996).
566 [53] G. Montes-Hernandeza et al., In-situ kinetic measurements of gas-solid carbonation of $Ca(OH)_2$
567 by using an infrared microscope coupled to a reaction cell, Chemical Engineering Journal 161 (2010)
568 250-256.

569 [54] C. Rodriguez-Navarro, K. Elert, R. Ševčík, Amorphous and crystalline calcium carbonate phases
570 during carbonation of nanolimes: implications in heritage conservation, Cryst Eng Comm. 18 (2016)
571 6594-6607.
572 [55] K.K. Sand et al., Crystallization of $CaCO_3$ in Water-Alcohol Mixtures: Spherulitic Growth,
573 Polymorph Stabilization, and Morphology, Cryst. Growth Des. 12 (2012) 842−853.